Bioresource Technology 261 (2018) 265–271

Contents lists available at ScienceDirect

Bioresource Technology

journal homepage: www.elsevier.com/locate/biortech

Investigating the adsorption behavior and the relative distribution of Cd^{2+} sorption mechanisms on biochars by different feedstock

Rong-Zhong Wang[a,b], Dan-Lian Huang[a,b,*], Yun-Guo Liu[a,b], Chen Zhang[a,b], Cui Lai[a,b], Guang-Ming Zeng[a,b], Min Cheng[a,b], Xiao-Min Gong[a,b], Jia Wan[a,b], Hao Luo[a,b]

[a] College of Environmental Science and Engineering, Hunan University, Changsha 410082, People's Republic of China
[b] Key Laboratory of Environmental Biology and Pollution Control (Hunan University), Ministry of Education, Changsha 410082, People's Republic of China

ARTICLE INFO

Keywords:
Biochar
Cadmium
Adsorption mechanism
Feedstock
Heavy metal

ABSTRACT

The objective of this study was to investigate the adsorption behavior and the relative distribution of Cd^{2+} sorption mechanisms on biochars by different feedstock. Bamboo biochars (BBCs), corn straw biochars (CBCs) and pig manure biochars (PBCs) were prepared at 300–700 °C. Adsorption results showed PBCs have the best adsorption capacity for Cd^{2+}, the extra adsorption capacity of PBCs mainly attributed to the precipitation or cation exchange, which played an important role in the removal of Cd^{2+} by PBCs. The contribution of involved Cd^{2+} removal mechanism varied with feedstock due to the different components and oxygen-containing functional groups. Cd^{2+}-π interaction was the predominant mechanism for Cd^{2+} removal on biochars and the contribution proportion significantly decreased from 82.17% to 61.83% as the ash content increased from 9.40% to 58.08%. Results from this study may suggest that the application of PBC is a feasible strategy for removing metal contaminants from aqueous solutions.

1. Introduction

Cadmium, one of the most toxic heavy metals (Gong et al., 2017a,b), has become a significant concern due to its high mobility and biological accumulation (Gong et al., 2017a), which could lead to bone and kidney damage after prolonged exposure(Gong et al., 2018; Huang et al., 2017a; Huang et al., 2017b; Huang et al., 2016a). Numerous techniques have been applied to eliminate Cd^{2+} from aqueous solutions, including chemical precipitation, membrane, ion exchange and adsorption, etc (Cheng et al., 2016a; Huang et al., 2016b; Xue et al., 2017; Zeng et al., 2017). Among these methods, adsorption is considered the most attractive method because of its low cost and environment-friendly (Cui et al., 2016). Several adsorbents have been widely applied to remove Cd^{2+} from aqueous solution, e.g., activated carbon, chitosan and organic material (Zhuang et al., 2016), while most of the adsorbents have disadvantage of either low efficiency, or disposal restrictions.

Biochar, a carbon-rich solid obtained by pyrolyzing pristine biomass material with no or limited oxygen, has attracted increasingly attention owing to its advantage of simple-design, and low-cost (Cui et al., 2016; Huang et al., 2017c; Huang et al., 2017d; Zhang et al., 2016). Due to its high specific surface area, abundant surface functional groups and porous structure, biochar exhibits a great potential to adsorb heavy metal (Nan et al., 2017). Many mechanisms were involved in heavy metal removal by biochars, including (i) precipitates with minerals (e.g., PO_4^{3-}, CO_3^{2-}); (ii) metal ion exchange (such as K^+, Ca^{2+}, Na^+, Mg^{2+}, -COOM, -R-O-M); (iii) surface complexation between metal cation and oxygen-containing functional groups (OFGs, e.g., –OH, -R-OH, –COOH); and (iv) coordination of metal cation with π electrons (e.g., C═C, C≡C) (Cui et al., 2016). The different mechanism and the relative contribution of these involved mechanisms largely depend on the feedstock and the pyrolysis conditions. Feedstock type has a significant influence on physicochemical properties of biochar. And the chemical compositions of biochar such as oxygen-containing functional groups, carbon fractions with aromatic structure and mineral constituents are also greatly controlled by the feedstock. So, the feedstock affect the adsorption process and associated mechanisms (Tag et al., 2016). Some researches have focused on the effects of feedstock on the adsorption capacity of biochars (Arán et al., 2016). However, till now, few studies have been performed to provide and compare the quantitative information regarding the relative contribution of these mechanisms on biochars by different feedstock.

So far, there are many investigations study on the removal of Cd^{2+} by different feedstock biochars, including peanut husk, *Canna indica,* and *Eichornia crassipes*, etc (Cheng et al., 2016b; Cui et al., 2016; Zhang et al., 2015). However, there are few researches on the investigation

* Corresponding author at: College of Environmental Science and Engineering, Hunan University, Changsha, Hunan 410082, People's Republic of China.
E-mail address: huangdanlian@hnu.edu.cn (D.-L. Huang).

https://doi.org/10.1016/j.biortech.2018.04.032
Received 8 February 2018; Received in revised form 2 April 2018; Accepted 7 April 2018
Available online 10 April 2018
0960-8524/

and comparison of the adsorption capacity and relative distribution of Cd^{2+} sorption mechanisms on biochar derived from corn straw (grass biomass), pig manure (live manure) and bamboo (woody plant). Biochars consist of the organic fractions and inorganic fractions. And the different fractions play different roles in the adsorption of heavy metal. For example, the organic fractions involved in the removal of heavy metal by oxygen-containing functional groups and cation-π interactions. The inorganic fractions removed heavy metal by precipitation or cation exchange. Researches demonstrated (Kołodyńska et al., 2012; Wang & Yan, 2011; Zhao et al., 2017) that the corn straw and bamboo derived biochars contain a lot of organic matter and a small part of ash content (< 10%), while the pig manure derived biochars often contain higher ash content (> 45%). So the adsorption capacity and the relative contribution of mechanisms of grass biomass or woody plant may be different from the livestock manure. The comparative study could provide an insight to discuss the role of involved mechanisms in the removal of heavy metal by different biochar. Thus, the pig manure (live manure), bamboo (woody biomass) and corn straw (grass biomass) derived biochars were choosed to study the adsorption capacity for Cd^{2+} and the effect of feedstock on the relative contribution of Cd^{2+} sorption mechanisms.

In this research, pig manure, bamboo and corn straw derived biochars have been prepared by oxygen-limited pyrolysis at 300–700 °C for the removal of Cd^{2+} from aqueous solution, and the objectives were to: (1) determine and compare the adsorption capacity of Cd^{2+} on biochars; (2) discuss the possible adsorption mechanisms of Cd^{2+}; and (3) investigate the contribution of different mechanisms by biochars.

2. Materials and methods

2.1. Preparation of biochars

Pig manure, bamboo and corn straw were taken from local farmers, washed and dried at room temperature, and then smashed to pass through a 100-mesh sieve (0.147 mm). Then the ground pig manure, bamboo and corn straw were pyrolyzed at 300, 500, and 700 °C under oxygen-limited conditions in a OTF-1200X-L tubular furnace with a heating rate of approximately 8 °C min^{-1}. Finally, the biochars were stored in scintillation vials with polypropylene caps and polyethylene liners in the dark until required for the adsorption experiment. The resulting biochars were abbreviated as BC300, BC500 and BC700 respectively, according to the pyrolysis temperature. The biochars prepared via three different feedstocks are named pig manure biochar (PBC), bamboo biochar (BBC) and corn straw biochar (CBC), respectively.

2.2. Batch sorption experiment

The Cd^{2+} solution was prepared using $Cd(NO_3)_2{\cdot}4H_2O$ (Guaranteed reagent, Sigma-Aldrich, USA). All the tested Cd^{2+} solutions contained 5 mM $NaNO_3$ as the background electrolyte. Adsorption experiments were conducted by adding 0.02 g biochars to 20 mL Cd^{2+} solution in vials at 25 °C. And the desired pH was adjusted to 5.0 ± 0.05 by either 0.1 M HNO_3 or NaOH solution. The effect of pH on Cd^{2+} adsorption by biochar was carried out by adjusting the initial pH from 2.0 to 7.0. For kinetic experiment, 100 mg L^{-1} Cd^{2+} solutions were shaken for different time interval (10 s, 20 s, 30 s, 60 s, 90 s, 2 min, 4 min, 8 min, 15 min, 40 min, 60 min, 120 min and 240 min). Adsorption isotherms were designed with the initial Cd^{2+} concentration in the range of 2–300 mg L^{-1}. In addition, 1 M NaCl, NH_4Cl, $CaCl_2$ and $AlCl_3$ were separately added to the mixture of Cd^{2+} and biochar suspension to investigate the effect of ionic strength on the sorption capacity. All vials were shaken at 180 rpm for 24 h. Once the adsorption experiment was completed, the mixtures were collected and filtered through 0.48 μm pore size nylon filters, and the concentration of Cd^{2+} in the filtrate was determined by Atomic Flame Absorption Spectrometer. The adsorption capacity Q (mg·g^{-1}) and the removal efficiency of Cd^{2+} on biochars, were calculated according to the following equation, respectively:

$$Q = (C_0 - C_e) * V / m \quad (1)$$

$$Adsorption\% = (C_0 - C_e)/C_0 \quad (2)$$

where C_e and C_0 are the equilibrium and the initial Cd^{2+} concentrations (mg·L^{-1}), respectively. V is the volume of solution (mL) and m is the weight of added biochar (g).

2.3. Sorption mechanisms

2.3.1. Biochar characterization

Various characterization methods were used to study the physical properties of different feedstocks biochars. Ash content was measured by heating the biochars in a muffle furnace at 750 °C for 6 h. The pH value of biochar samples was determined by mixing biochar to deionized water at a ratio of 1:10 (w/v). The zeta potential of biochar at varying solution pH from 2.0 to 7.0 was determined by Electroacoustic Spectrometer (Mastersizer 2000). Furthermore, the surface area, pore size and pore volume were measured by 3Flex Surface Characterization Analyzer (Micromeritics Instrument Corporation). The surface functional groups of materials were determined X-Ray Photoelectron Spectroscopy (XPS) (Zhou et al., 2017). X-ray Powder Diffraction (XRD-6100) was primarily used for identifying the crystalline constituents of different chemical modified biochars.

2.3.2. Quantitative analysis of different mechanisms to Cd^{2+} sorption

According to the calculation method (Zhang et al., 2017a), the sorption capacity attributed to three fractions: i) precipitation or cation exchange with minerals (Q_p); The reduced amount of Cd^{2+} sorption on the biochars before and after acid-washed was an indicator for the calculation of minerals effect (Cui et al., 2016). After acid-washed, most of ash from the biochar was removed, and the oxygen containing functional groups were not changed. The sorption attributed to the interaction with minerals (Q_p) was calculated as Eq. (3); ii) oxygen functional groups(OFGs)complexation (Q_f). A drop of pH before and after Cd^{2+} sorption on acid-washed biochars was observed, which was resulted from the complication with the oxygen-containing organic groups, which was reported in a previous paper (Wang et al., 2015b). It could be described as the following reaction modes (4) and (5).

$$-COOH + Cd^{2+} + H_2O \rightarrow -COOHCd^{+} + H_3O^{+} \quad (4)$$

$$-OH + Cd^{2+} + H_2O \rightarrow -OCd^{+} + H_3O^{+} \quad (5)$$

iii) coordination of heavy metals with π electrons (Cd^{2+}-π) interaction (Q_π). Cd^{2+} sorption on acid-washed biochars was the sum of the Cd^{2+}-π interaction and functional group complexation together. Therefore, the amount of Q_π could be calculated as shown in Eq. (6). (Cui et al., 2016) The contribution percentage of different mechanisms to the overall Cd^{2+} sorption was then calculated using the Q_f/Q_t, Q_p/Q_t and Q_p/Q_t ratio.

$$Q_p = Q_t - Q_a \quad (3)$$

$$Q_\pi = Q_a - Q_f \quad (6)$$

where Q_p is the amount of Cd^{2+} sorption attributed to the precipitation or cation exchange with minerals, Q_t is the total sorption of Cd^{2+} on biochar, Q_a is the amount of adsorbed Cd^{2+} on biochar after the acid dipping procedure, Q_π is the amount of Cd^{2+} sorption resulting from Cd^{2+}-π interaction, and Q_f is the oxygen functional groups complications.

3. Results and discussion

3.1. Adsorption study

3.1.1. Kinetic study

The comparison of Cd^{2+} sorption characteristics by CBC, PBC and BBC were performed by varying time from 10 s to 240 min. Cd^{2+} removal by all biochars exhibited initial high removal efficiency within 2 min, and then reached the equilibrium in 60 min with a small variation (see Supplementary material). For CBC samples, CBC700 exhibited best adsorption performance and the removal efficiency reached 76.02% in 60 min. In the case of PBC samples, PBC700 showed a good adsorption capacity and the sorption amount of PBC700 reached 74.42 mg g^{-1} in 2 min, which accounted for 94.07% to its total amount of adsorption. After quick adsorption, PBC700 removed about 79.11% of Cd^{2+}, with final adsorption capacity of 79.11 mg g^{-1}. In the BBC sample, Cd^{2+} was rapidly adsorbed 74.39 mg g^{-1} onto BBC700 within 2 min, which accounted for 97.02% to their total amount of adsorption, respectively, while the rate of Cd^{2+} sorption in the next 60 min became slower and only accounted for 2.98% to their total amount of adsorption. At the end of adsorption process, the removal efficiency of BBC700 reached 76.65%. In the cases of CBC700, PBC700 and BBC700, the time of reaching the equilibrium state was similar and the adsorption capacity followed the order: PBC700 > BBC700 > CBC700. The differences in kinetics between CBC, PBC and BBC were correlated with the different physico-chemical characteristics of these biochars. PBC700 was characterized with a higher content of ash than BBC700 and CBC700, which was beneficial to the removal of heavy metal through a complex mechanism involving surface adsorption, precipitation and ion exchange (Zhang et al., 2017a,b). Moreover, the pore volume of PBC700 is 4.29 times and 2.14 times of that of BBC700 and CBC700, respectively. So, PBC700 exhibited the best adsorption performance for Cd^{2+}.

To explore the underlying mechanisms of the adsorption for Cd^{2+} by biochars, pseudo first order kinetic equation and pseudo second order kinetic model were employed to describe the kinetics of Cd^{2+} sorption on biochars. Two kinetics models can be expressed as Eqs. (7) and Eqs. (8) (Zhou et al., 2016):

$$\ln(Q_e - Q_t) = \ln Q_e - k_1 t \quad (7)$$

$$t/Q_t = 1/k_2 Q_e^2 + t/Q_e = 1/h + t/Q_e \quad (8)$$

where Q_t (mg g^{-1}) represents the amount adsorbed of Cd^{2+} at time t and Q_e (mg g^{-1}) at equilibrium; k_1 (min^{-1}) and k_2 (g mg^{-1} min^{-1}) are the rate constant of pseudo-first order and pseudo-second-order which can be calculated from the plot of ln ($Q_e - Q_t$) versus t and t/Q_t versus t, respectively; h represents the initial sorption rate (mg g^{-1} min^{-1}).

The calculated results of first-order and second-order rate equations are shown in Table 1. For CBC, PBC and BBC samples, the values of the regression coefficient (R^2) calculated based on the pseudo-second-order kinetic model are larger than the pseudo-first-order kinetic model, indicating the pseudo-second-order model could preferably describe the adsorption process in this study. Based on pseudo-second-order model assumption, the mechanism of heavy metal adsorption was limited by bonding forces through sharing or ion/electrons exchange between adsorbate and adsorbent. While the pseudo-first-order model assumes that the diffusion of adsorbate dominants the adsorption velocity (Nan et al., 2017). Thus, the result indicated that chemical process may be the rate-limiting step in the adsorption process for Cd^{2+}.

Table 1
Kinetic parameters of the pseudo-first-order and pseudo-first-order equations for Cd^{2+} adsorption onto biochars by different feedstock.

Sorbent	Pseudo-first-order			Pseudo-second-order		
	Q_e (mg g^{-1})	k_1	R_{adj}^2	Q_e (mg g^{-1})	$K_2 \times 10^2$	R_{adj}^2
CBC300	70.44	1.66	0.9843	72.47	2.50	0.9860
CBC500	72.40	1.64	0.9744	74.70	2.47	0.9847
CBC700	73.32	1.81	0.9822	75.62	2.81	0.9929
PBC300	76.08	1.48	0.9795	78.16	2.32	0.9838
PBC500	76.60	1.51	0.9842	78.68	2.40	0.9870
PBC700	77.34	1.55	0.9867	79.43	2.52	0.9882
BBC500	72.25	1.95	0.9841	74.35	3.10	0.9889
BBC500	72.57	2.00	0.9851	74.65	3.25	0.9910
BBC700	73.45	2.14	0.9782	75.26	3.75	0.9783

3.1.2. Isotherm study

Batch experiments were carried out by varying the concentration of Cd^{2+} from 2 to 300 mg L^{-1} to study adsorption isotherms. To further explaining the adsorption mechanism of Cd^{2+} onto biochar surfaces, Langmuir and Freundlich models were used to fit the Cd^{2+} adsorption isotherm data. Langmuir isotherm focused on this assumption that the surface of the adsorbent is uniform and no interactions between adsorbate molecules on adjacent sites exist, and the linearized form of this isotherm is expressed as follows (Cheng et al., 2016a):

$$Q_e = K_L Q_m C_e/(1 + K_L C_e) \quad (9)$$

$$R_L = 1/(1 + C_0 K_L) \quad (10)$$

where Q_m (mg g^{-1}) is the maximum absorption capacity; Q_e (mg g^{-1}) and C_e (mg L^{-1}) are the amount of adsorbed Cd^{2+} and Cd^{2+} concentration in the solution at equilibrium, respectively, C_0 (mg L^{-1}) is the lowest initial concentration of Cd^{2+} in the solution, and K_L is the affinity constant. R_L was classified to determine whether the adsorption process is favorable for the Langmuir type adsorption process.

Freundlich isotherm assumes that metal ions uptake occurs on a heterogeneous surface by multilayer adsorption, the empirical nonlinear equation and sorption distribution coefficient equation can be written as follows (Uçar et al., 2014):

$$Q_e = K_F C_e^{1/n} \quad (11)$$

where K_F (mg g^{-1}) and n are the adsorption equilibrium constant.

It can be observed that Langmuir isotherm model fitted the equilibrium data better than the Freundlich model (Fig. 1), suggesting that chemisorption of Cd^{2+} may occur on the homogeneous surfaces of biochars and the chemisorption is monolayer adsorption (Cui et al., 2016). Furthermore, the values of R_L are found in the range of 0.9259–0.9456 for Cd^{2+} onto different biochars, indicating that sorption of Cd^{2+} on these biochars was favorable under the experimental condition.

The values of Q_m and K_d ($K_d = Q_e/C_e$) were calculated to evaluate their sorption capacities at different Cd^{2+} equilibrium concentration. The values of K_d and Q_m both followed this order: PBC700 > BBC700 > CBC700, which confirmed the strong sorption affinity of PBC700. Furthermore, compared with other biochars, such as *Canna indica* biochars (63.32–140.01 mg g^{-1}) (Cui et al., 2016), the biogas production residue biochar (32.57–76.34 mg g^{-1}) (Bogusz et al., 2017), rape straw biochars 32.74–81.10 mg g^{-1}) (Li et al., 2017), aminothiourea chitosan modified magnetic biochar composites (93.72–137.3 mg g^{-1}) (Li et al., 2018), and the ferromanganese binary oxide-biochar composites (101.0 mg g^{-1}) (Zhou et al., 2018), the Q_m values of pig manure biochar (212.51–240.23 mg g^{-1}) were larger than these biochars, suggesting that pig manure biochars would be applicable for the removal of Cd^{2+}. In addition, compared with other material, the cost of the PBC is much lower (see Supplementary material). Moreover, the K_d values for BC300, BC500 and BC700 greatly decreased with increasing Cd^{2+} concentration, because Cd^{2+} sorption on the biochars was nonlinear (Zhou et al., 2016). The difference of Cd^{2+} sorption affinity on these biochar was possibly due to the morphology, structure and content of functional groups in these biochars.

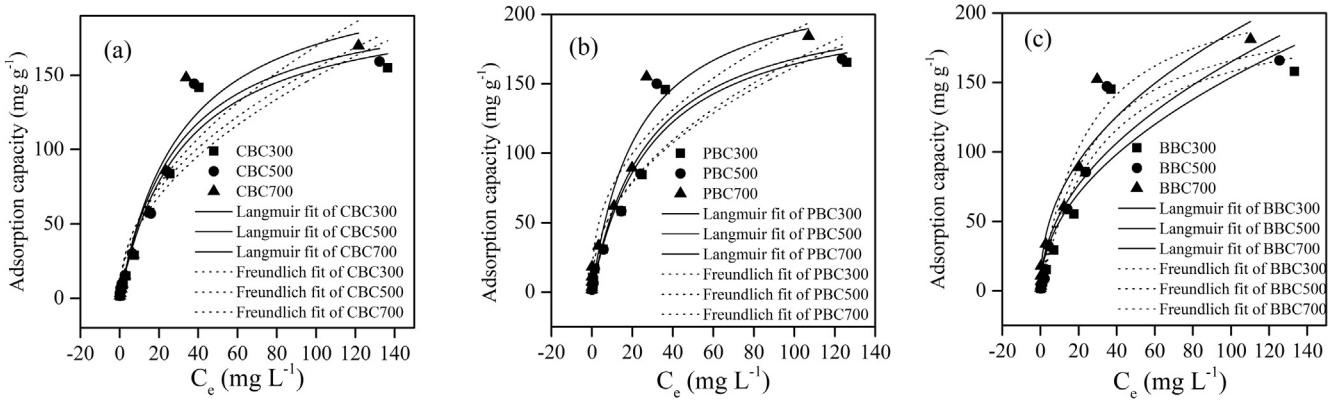

Fig. 1. Adsorption isotherms of Cd^{2+} on different biochars. (initial Cd^{2+} concentration = 2–300 mg L^{-1}; sorbent dose = 1 g L^{-1}; contact time = 24 h).

3.1.3. Effect of initial pH on Cd^{2+} adsorption

pH is one of the most critical factors in Cd^{2+} sorption since it may influence the charge on the surface of material and the degree of ionization and speciation of pollutant (Lai et al., 2016; Wang et al., 2016). To evaluate the effect of solution pH value on Cd^{2+} adsorption, adsorption experiments were carried out within a range of pH 2.0–7.0. As illustrated in Figs. 2–4, for BC samples, the amount of Cd^{2+} sorption increased with increasing of initial pH from 2.0 to 5.0, which was related to the surface charge of the adsorbent at different pH solution. The isoelectric point (IEP) of the CBC700, PBC700, BBC700 were achieved at approximately pH 2.0–3.0. When the solution pH was 2.0, which was lower than pH_{pzc} of BC, the surface of BC was protonated and caused greater electrostatic repulsion to the positively charged Cd^{2+}. When pH > pHpzc, the surface of BC was deprotonated, so the electrostatic attraction increases between the adsorbent and metal, then increase adsorption capacity (Yap et al., 2016). Electrostatic interactions originated from sorbent surface and cationic are likely the driving force for Cd^{2+} sorption on biochar surfaces. However, PBC700 with minor surface charge exhibited greater sorption for Cd^{2+} than CBC700 and BBC700, indicating that electrostatic interactions were not the only driving force. As showed in Figs. 2–4 (b, c), due to the addition of biochar, the pH of the equilibrium solution increased as compared with the initial pH. Biochar generally has an alkaline pH, which could neutralize the solution acidity. Nevertheless, compared with the system without Cd^{2+} (Figs. 2–4 (c)), the pH of equilibrium solution was lower when Cd^{2+} was added and sorbed onto biochar (Figs. 2–4 (b)). Cui (2016) deemed that the reduction of solution pH was connected to the coordination between the OFGs (e.g., ACOOH and AOH) and heavy metal ion, which was usually accompanied with the release of H^+. In addition, the decrease in solution pH after Cd sorption may also result from the formation of the Cd precipitate with alkali ions (e.g., PO_4^{3-}, CO_3^{2-}) (Cui et al., 2016; Wnetrzak et al., 2014). These results indicated electrostatic interactions, precipitation and coordination were involved in the Cd^{2+} adsorption.

3.1.4. Effect of ionic strength on Cd^{2+} adsorption

Taken into account the fact that many cations universally existed in actual industrial wastewater and polluted groundwater, and the presence of these cations may interfere in the removal efficiency of Cd^{2+} (Dong et al., 2010). The effects of Na^+, Ca^{2+}, and Al^{3+} on the Cd^{2+} adsorption by biochars were tested. The metal ions generally decreased the removal efficiency of Cd^{2+} on biochars, and the inhibitory effect order is: Al^{3+} > Ca^{2+} > Na^+ (see Supplementary material). The inhibitory effect may be ascribed to the fact that metal ions compete for the same adsorption sites (Wang et al., 2015a). Ionic strength (I) dependence is generally applied to distinguish inner-sphere (I independent) and outer-sphere (I dependent) sorption mechanisms (Uchimiya, 2014). In the inner-sphere sorption mechanisms, cations would not compete for the inner-sphere sites. In the outer-sphere sorption mechanisms, cations such as Na^+, Ca^{2+} and Al^{3+} could compete with the target ions to form outer-sphere surface complexes and subsequently reduced the adsorption efficiency of target ion (Guo et al., 2008). Thus, the result suggested that some Cd^{2+} adsorbed on the outer-sphere sorption sites.

3.2. Possible mechanisms for Cd^{2+} adsorption on biochars

According to the above results, the adsorption behaviors of the different feedstock biochars for Cd^{2+} were different. The differences were correlated with the physico-chemical characteristics of these biochars. Table 2 listed physical properties of CBC700, PBC700, BBC700. As shown, PBC700 exhibited a good porous structure, the pore volume of which is 2.14 times as large as CBC700, 4.29 times as much as BBC700. According to the adsorption results, PBC700 displayed best adsorption performance than BBC700 and CBC700, suggesting that big pore volume may beneficial to heavy metal removal. Besides that, the surface area and pore volume of CBC700 was 1.93 and 2 times respectively as large as BBC700, whereas the adsorption capacity is slightly lower than that of BBC700, which indicated chemical process

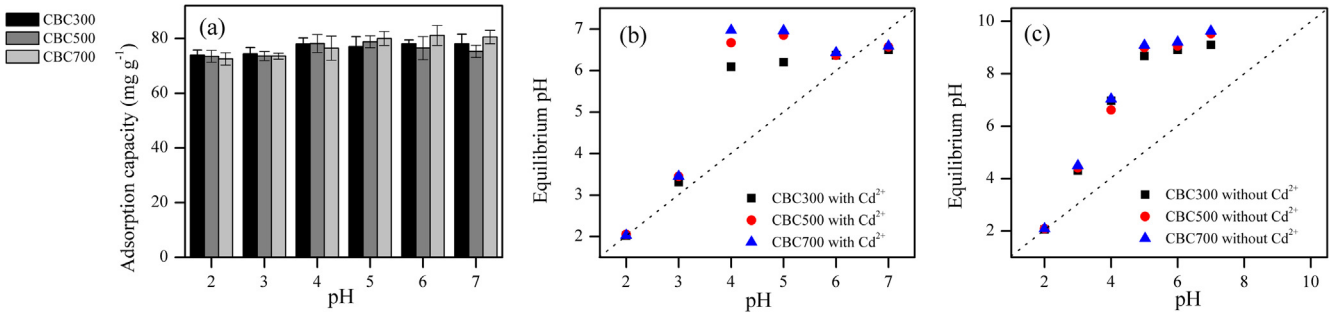

Fig. 2. (a) Effect of pH on Cd^{2+} sorption by CBCs. (b) The pH values change of the mixed solution of CBCs with Cd^{2+} after equilibration. (c) The pH values change the mixed solution of CBCs without Cd^{2+} after equilibration.

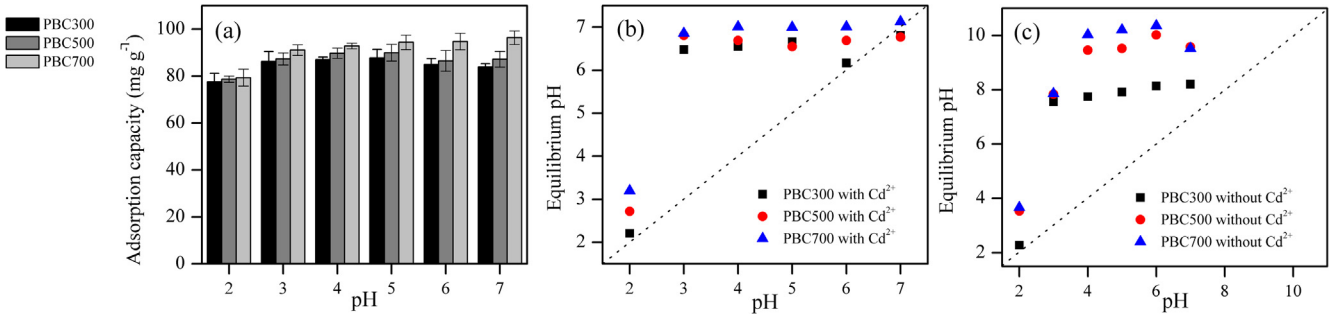

Fig. 3. (a) Effect of pH on Cd^{2+} sorption by PBCs. (b) The pH values change of the mixed solution of PBCs with Cd^{2+} after equilibration. (c) The pH values change the mixed solution of PBCs without Cd^{2+} after equilibration.

may play an important role in the adsorption process of Cd^{2+}. The pH values of these biochars were high due to the high pyrolysis temperature. Furthermore, the ash content of theses biochars followed this order: PBC700 > CBC700 > BBC700, which is different from the adsorption capacity order: PBC700 > BBC700 > CBC700, suggesting that ash content play a role but not an important role in the removal of heavy metal.

XPS was applied to characterization of the oxygen-containing function groups on surface of biochars. The XPS C1s peaks of CBC700, BBC700, and PBC700 clearly showed that the oxygen containing groups were prevalent on the outer surface of biochars (see Supplementary material). The C1s spectra were resolved into four component peaks with binding energy 284.6 eV, 285.3 eV, 287.3 8 eV and 289.7 eV, which attached to the C–C, C-O, C═O and O-C═O, respectively. PBC700, BBC700 and CBC700 all contained three oxygen-containing functional groups, while the ratios of different biochars were different. It was found that the ratio of O-C═O in PBC700 was the maximum, which was 1.79 times as large as CBC700, 6.30 times as much as BBC700. Previous research has indicated O-C═O was beneficial to heavy metal (Chen et al., 2015), which was consistent with the above adsorption experiment.

To give insights into the mechanism of Cd^{2+} adsorption, XPS was used to analyze the changes in binding energy of C 1 s and O 1 s in PBC700 biochar before and after adsorption. C 1 s spectra showed that the binding energy of the peaks (C═O, C-O and C–C) has a certain degree of shift after Cd^{2+} adsorption (see Supplementary material). It was found that the ratio of O-C═O decreased from 15.68% to 2.73% after Cd^{2+} adsorption, indicating that the O-C═O groups had been largely consumed by Cd^{2+}. After Cd^{2+} being absorbed, the quantity of C═O groups increased (from 10.93% to 12.47%), whereas that the C-O decreased from 40.25% to 32.94%. This result was consistent with the previous study by Chao et al., (Zhang et al., 2017a). Similarly, four characteristic peaks were identified for the O 1 s spectrum in PBC700 before and after Cd^{2+} adsorption (Fig. 4(e–f)). It showed that the ratio of metal oxide increased from 4.64% to 7.22%, suggesting the formation of Cd-O on the surface of biochar. (Zhang et al., 2017a). Besides

Table 2
Physicochemical properties of CBC700, PBC500 and BBC700.

Biochars	pH	Ash content (%)	Surface Area ($m^2\ g^{-1}$)	Pore Volume ($cm^3\ g^{-1}$)	Pore Size (Å)
CBC700	10.36	9.40	13.10	0.014	27.74
PBC700	10.92	58.08	11.37	0.030	44.73
BBC700	10.33	5.05	6.79	0.007	25.96

that, the peak of area of C═O increased from 51.54% to 54.69%. The peak of C-O (alcoholic hydroxyl, and/or ether) after adsorption is less than that before adsorption (13.21% vs 10.43%). These are consistent with the findings from the C1s spectra. XPS result indicated participation of phenolic hydroxyl and carboxylic groups in Cd^{2+} sorption by biochars (Zhuang et al., 2016), and surface complexation was involved in the Cd^{2+} adsorption.

The deconvolution of XPS bands, which give the precise binding energies of Cd^{2+} after adsorption. The Cd spectrum was resolved into two component peaks with binding energy 405.8 eV and 412.6 eV (see Supplementary material). The peak at 412.6 eV can be connected to Cd-O, which implied Cd^{2+} is bonded to OFGs on the surface of biochars. And the ratio of Cd-O was 37.32%. The peak at 405.8 eV can be associated with Cd-π interaction, suggesting Cd^{2+} binding to electron-rich domains of graphene-like aromatic structures. The ratio of Cd-π interaction was 62.68%, indicating Cd-π interaction was predominant sorption mechanism. These results are consisted with phyllostachys pubescens biochar for the removal of Cd^{2+} (Trakal et al., 2015).

To further explore the Cd^{2+} removal mechanism, original and Cd^{2+}-loaded PBC700 samples were comparatively analyzed with SEM, EDX, XPS and XRD (see Supplementary material). Compared with the original biochar, a larger number of granular crystals were observed in the SEM image of Cd-loaded biochars (PBC700 + Cd), and their elemental composition are further investigated by EDX spectrum. Likewise, these precipitates of PBC700 were identified with typical peaks the XRD patterns. The remarkable peak of Cd was detected for the PBC700 sample, implying Cd^{2+} successfully adsorbed on the surface of

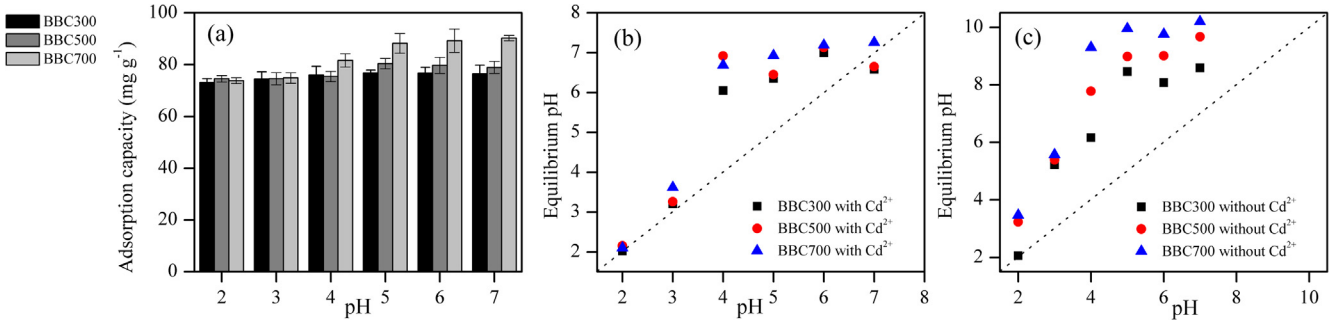

Fig. 4. (a) Effect of pH on Cd^{2+} sorption by BBCs. (b) The pH values change of the mixed solution of BBCs with Cd^{2+} after equilibration. (c) The pH values change the mixed solution of BBCs without Cd^{2+} after equilibration.

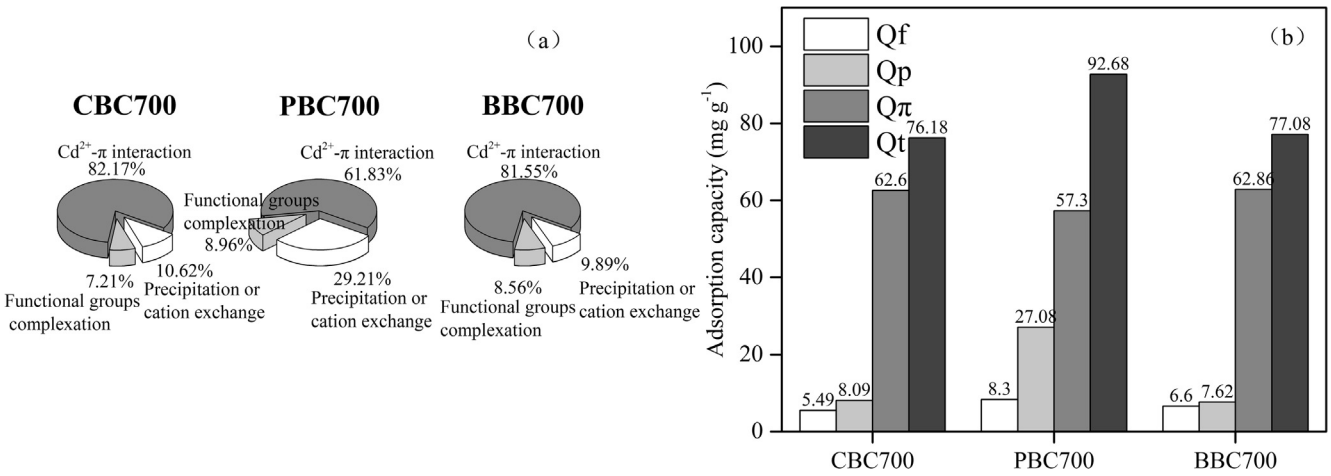

Fig. 5. The contribution percentage of different mechanisms to the overall Cd^{2+} adsorption on biochars (a) and the estimated contribution of Cd^{2+} sorption on biochars (b).

biochar. Moreover, Cd^{2+} loaded on PBC700 was demonstrated by a prominent of Cd3d peak in the overall XPS spectrum after Cd^{2+} sorption. To further explore the Cd precipitate, XRD was used to analyze original and Cd^{2+}-loaded PBC700 samples. As indicated by XRD (see Supplementary material), several new peaks appeared in Cd^{2+}-loaded PBC700 samples, which associated with $CdCO_3$, Cd_3P_2 and $Cd_3(PO_4)_2$, respectively. This result was consistent with the previous study by Zhang et al. (2015). These precipitates formed in Cd^{2+}-loaded biochars may be attributed to precipitation between Cd^{2+} and the dissolved anions (e.g., PO_4^{3-}, CO_3^{2-}) from the minerals in biochars.

3.3. Quantitative analysis of different mechanisms to Cd^{2+} adsorption

According to the adsorption of Cd^{2+} on original biochar and demineralized biochars, the contribution of different mechanisms to the Cd^{2+} could be calculated. The contributions of OFGs complexation (Q_f), Cd^{2+}-π interaction (Q_π) and precipitation or cation exchange with minerals (Q_p) are showed in Fig. 5(a). For BBC and CBC samples, Cd^{2+}-π interaction contribute above 80% in the total adsorption capacity, the precipitation or cation exchange account for 10%, and the contribution of OFGs complexation was only 7.21–8.56%. Due to the ratio of ash content and OFGs was small, the contribution of precipitation or cation exchange and OFGs complexation also very little. Besides, because of the ratio of ash content in the CBC700 was higher than BBC700, the contribution of precipitation or cation exchange in CBC700 was higher than BBC700. In the case of PBC sample, the ratio of Cd^{2+}-π interaction in the involved mechanism decreased significantly (61.83%) compared to BBC700 and CBC700 (81.55%–82.17%), while the contribution proportion of precipitation or cation exchange increased to 29.21%, which mainly attributed to the higher ash content (58.08%). And the contribution of OFGs complexation by PBC700 was higher than BBC700 and CBC700.

In general, for all biochar samples, the contribution for Cd^{2+} adsorption followed the order: $Q_\pi > Q_p > Q_f$, which was consistent with the Zhang's study (2017a,b). For Q_f, the ratio is much lower than Q_π and Q_p, which may be explained by that high pyrolysis temperature decreased the amount of OFGs and then decreased the surface complexation. Wang et al. (2015b) demonstrated this conjecture. For Q_p, the contribution of Q_p increased from 9.89% to 29.21% as the ash content of biochars increased from 5.05% to 58.08%. For Q_π, their values were up to 57.30–62.86 mg g^{-1}, accounting for 61.83–82.17% of the Q_t values (Fig. 5(a)), suggesting that Cd^{2+}-π interaction played a dominant role in Cd^{2+} adsorption.

Furthermore, as shown in Fig. 5(b), the adsorption capacity of Cd^{2+} for PBC700, CBC700, BBC700 was 92.68, 76.18, 77.08 mg g^{-1}, respectively. Among them, about 57.3–62.86 mg g^{-1} was attributed to the organic fractions of biochars which involved in surface complexation and Cd^{2+}-π interaction. The ash content which involved in precipitation or cation exchange only contribute 7.62–27.08 mg g^{-1} to the total adsorption capacity. In addition, especially for PBC700, the ratio of ash content in the biochar was about 58%, while the contribution of precipitation or cation exchange in the total adsorption capacity was only 29%, further demonstrated that the organic fractions played a dominant role in the removal of heavy metal by biochars. On the other hand, with the increased of ratio of ash content, the adsorption capacity of ash content increased, indicating that ash content also played an important role in the adsorption process. Moreover, as shown in Fig. 5(b), the excess adsorption capacity of PBC700 mainly attribute to the precipitation or cation exchange, also demonstrated that the ash content of pig manure derived biochar played an important role in removal of heavy metal.

4. Conclusions

Because of the different components and oxygen-containing functional groups, the contribution of involved mechanism on biochars varied with the feedstock. Cd^{2+}-π interaction was the predominant mechanism for Cd^{2+} removal on biochars. For biochars with pyrolysised at high temperature, oxygen-containing functional groups played a less important role in the removal of heavy metal. Live manure was more suitable as feedstock to prepare biochar for the removal of heavy metal than woody plant and grass biomass due to the higher adsorption capacity. And the ash content play an important role in the removal of heavy metal by live manure derived biochars.

Acknowledgements

This study was financially supported by the Program for the National Natural Science Foundation of China (51579098, 51408206, 51779090, 51521006, 51278176, 51378190), the National Program for Support of Top–Notch Young Professionals of China (2014), the Program for Changjiang Scholars and Innovative Research Team in University (IRT-13R17), and Hunan Provincial Science and Technology Plan Project (No. 2016RS3026, 2017SK2243), and the Fundamental Research Funds for the Central Universities (531107051080, 531107050978).

A competing interests statement

We declared that we have no competing interests.

Appendix A. Supplementary data

Supplementary data associated with this article can be found, in the online version, at https://doi.org/10.1016/j.biortech.2018.04.032.

References

Arán, D., Antelo, J., Fiol, S., Macías, F., 2016. Influence of feedstock on the copper removal capacity of waste-derived biochars. Bioresour. Technol. 212, 199–206.

Bogusz, A., Nowak, K., Stefaniuk, M., Dobrowolski, R., Oleszczuk, P., 2017. Synthesis of biochar from residues after biogas production with respect to cadmium and nickel removal from wastewater. J. Ind. Eng. Chem. 201, 268–276.

Chen, Z., Xiao, X., Chen, B., Zhu, L., 2015. Quantification of chemical states, dissociation constants and contents of oxygen-containing groups on the surface of biochars produced at different temperatures. Environ. Sci. Technol. 49 (1), 309–317.

Cheng, M., Zeng, G., Huang, D., Cui, L., Xu, P., Zhang, C., Liu, Y., 2016a. Hydroxyl radicals based advanced oxidation processes (AOPs) for remediation of soils contaminated with organic compounds: a review. Chem. Eng. J. 284, 582–598.

Cheng, Q., Huang, Q., Khan, S., Liu, Y., Liao, Z., Li, G., Yong, S.O., 2016b. Adsorption of Cd by peanut husks and peanut husk biochar from aqueous solutions. Ecol. Eng. 87, 240–245.

Cui, X., Fang, S., Yao, Y., Li, T., Ni, Q., Yang, X., He, Z., 2016. Potential mechanisms of cadmium removal from aqueous solution by Canna indica derived biochar. Sci. Total Environ. 562, 517–525.

Dong, L.J., Zhu, Z.L., Qiu, Y.L., Zhao, J.F., 2010. Removal of lead from aqueous solution by hydroxyapatite/magnetite composite adsorbent. Chem. Eng. J. 165 (3), 827–834.

Gong, X., Huang, D., Liu, Y., Peng, Z., Zeng, G., Xu, P., Cheng, M., Wang, R., Wan, J., 2017a. Remediation of contaminated soils by biotechnology with nanomaterials: bio-behavior, applications, and perspectives. Crit. Rev. Bio. 1–14.

Gong, X., Huang, D., Liu, Y., Zeng, G., Wang, R., Wan, J., Zhang, C., Cheng, M., Qin, X., Xue, W., 2017b. Stabilized nanoscale zero-valent iron mediated cadmium accumulation and oxidative damage of Boehmeria nivea (L.) Gaudich cultivated in cadmium contaminated sediments. Environ. Sci. Technol. 51 (19), 11308–11316.

Gong, X., Huang, D., Liu, Y., Zeng, G., Wang, R., Wei, J., Huang, C., Xu, P., Wan, J., Zhang, C., 2018. Pyrolysis and reutilization of plant residues after phytoremediation of heavy metals contaminated sediments: For heavy metals stabilization and dye adsorption. Bioresour. Technol. 253, 64–71.

Guo, X., Zhang, S., Shan, X.Q., 2008. Adsorption of metal ions on lignin. J. Hazard. Mater. 151 (1), 134–142.

Huang, D., Gong, X., Liu, Y., Zeng, G., Lai, C., Bashir, H., Zhou, L., Wang, D., Xu, P., Cheng, M., 2017a. Effects of calcium at toxic concentrations of cadmium in plants. Planta 245 (5), 1–11.

Huang, D., Guo, X., Peng, Z., Zeng, G., Xu, P., Gong, X., Deng, R., Xue, W., Wang, R., Yi, H., 2017b. White rot fungi and advanced combined biotechnology with nanomaterials: promising tools for endocrine-disrupting compounds biotransformation. Crit. Rev. Bio. 1–19.

Huang, D., Hu, C., Zeng, G., Cheng, M., Xu, P., Gong, X., Wang, R., Xue, W., 2016a. Combination of Fenton processes and biotreatment for wastewater treatment and soil remediation. Sci. Total Environ. 574, 1599–1610.

Huang, D., Liu, L., Zeng, G., Xu, P., Huang, C., Deng, L., Wang, R., Wan, J., 2017c. The effects of rice straw biochar on indigenous microbial community and enzymes activity in heavy metal-contaminated sediment. Chemosphere 174, 545–553.

Huang, D., Wang, X., Zhang, C., Zeng, G., Peng, Z., Zhou, J., Cheng, M., Wang, R., Hu, Z., Qin, X., 2017d. Sorptive removal of ionizable antibiotic sulfamethazine from aqueous solution by graphene oxide-coated biochar nanocomposites: Influencing factors and mechanism. Chemosphere 186, 414–421.

Huang, D., Xue, W., Zeng, G., Wan, J., Chen, G., Huang, C., Zhang, C., Cheng, M., Xu, P., 2016b. Immobilization of Cd in river sediments by sodium alginate modified nanoscale zero-valent iron: impact on enzyme activities and microbial community diversity. Water Res. 106, 15–25.

Kołodyńska, D., Wnętrzak, R., Leahy, J.J., Hayes, M.H.B., Kwapiński, W., Hubicki, Z., 2012. Kinetic and adsorptive characterization of biochar in metal ions removal. Chem. Eng. J. 197 (29), 295–305.

Lai, C., Wang, M.M., Zeng, G.M., Liu, Y.G., Huang, D.L., Zhang, C., Wang, R.Z., Xu, P., Cheng, M., Huang, C., 2016. Synthesis of surface molecular imprinted TiO_2/graphene photocatalyst and its highly efficient photocatalytic degradation of target pollutant under visible light irradiation. Appl. Surf. Sci. 390, 368–376.

Li, B., Yang, L., Wang, C.Q., Zhang, Q.P., Liu, Q.C., Li, Y.D., Xiao, R., 2017. Adsorption of Cd(II) from aqueous solutions by rape straw biochar derived from different modification processes. Chemosphere 175, 332.

Li, R., Liang, W., Huang, H., Jiang, S., Guo, D., Li, M., Zhang, Z., Ali, A., Wang, J.J., 2018. Removal of cadmium(II) cations from an aqueous solution with aminothiourea chitosan strengthened magnetic biochar. J. Appl. Polym. Sci. 46239.

Nan, Z., Chen, H., Xi, J., Yao, D., Zhi, Z., Yun, T., Lu, X., 2017. Biochars with excellent Pb (II) adsorption property produced from fresh and dehydrated banana peels via hydrothermal carbonization. Bioresour. Technol. 232, 204–210.

Tag, A.T., Duman, G., Ucar, S., Yanik, J., 2016. Effects of feedstock type and pyrolysis temperature on potential applications of biochar. J. Anal. Appl. Pyrol. 120, 200–206.

Trakal, L., Veselská, V., Šafarík, I., Vítková, M., Číhalová, S., Komárek, M., 2015. Lead and cadmium sorption mechanisms on magnetically modified biochars. Bioresour. Technol. 203, 318–324.

Uçar, S., Erdem, M., Tay, T., Karagöz, S., 2014. Removal of lead (II) and nickel (II) ions from aqueous solution using activated carbon prepared from rapeseed oil cake by Na_2CO_3 activation. Clean Technol. Environ. 17 (3), 747–756.

Uchimiya, M., 2014. Influence of pH, ionic strength, and multidentate ligand on the interaction of Cd II with biochars. Acs Sustain. Chem. Eng. 2 (8), 2019–2027.

Wang, H., Gao, B., Wang, S., Fang, J., Xue, Y., Yang, K., 2015a. Removal of Pb(II), Cu(II), and Cd(II) from aqueous solutions by biochar derived from KMnO4 treated hickory wood. Bioresour. Technol. 197, 356–362.

Wang, L.G., Yan, G.B., 2011. Adsorptive removal of direct yellow 161dye from aqueous solution using bamboo charcoals activated with different chemicals. Desalination 274 (1), 81–90.

Wang, R.Z., Huang, D.L., Liu, Y.G., Peng, Z.W., Zeng, G.M., Lai, C., Xu, P., Huang, C., Zhang, C., Gong, X.M., 2016. Selective removal of BPA from aqueous solution using molecularly imprinted polymers based on magnetic graphene oxide. RSC Adv. 6 (108), 106201–106210.

Wang, Z., Liu, G., Zheng, H., Li, F., Ngo, H.H., Guo, W., Liu, C., Chen, L., Xing, B., 2015b. Investigating the mechanisms of biochar's removal of lead from solution. Bioresour. Technol. 177, 308–317.

Wnetrzak, R., Leahy, J.J., Chojnacka, K.W., Saeid, A., Novotny, E., Jensen, L.S., Kwapinski, W., 2014. Influence of pig manure biochar mineral content on Cr(III) sorption capacity. J. Chem. Technol. Biot. 89 (4), 569–578.

Xue, W., Huang, D., Zeng, G., Wan, J., Zhang, C., Xu, R., Cheng, M., Deng, R., 2017. Nanoscale zero-valent iron coated with rhamnolipid as an effective stabilizer for immobilization of Cd and Pb in river sediments. J. Hazard. Mater. 341, 381–389.

Yap, M.W., Mubarak, N.M., Sahu, J.N., Abdullah, E.C., 2016. Microwave induced synthesis of magnetic biochar from agricultural biomass for removal of lead and cadmium from wastewater. J. Ind. Eng. Chem. 45, 287–295.

Zeng, G., Jia, W., Huang, D., Liang, H., Chao, H., Min, C., Xue, W., Gong, X., Wang, R., Jiang, D., 2017. Precipitation, adsorption and rhizosphere effect: the mechanisms for Phosphate-induced Pb immobilization in soils-A review. J. Hazard. Mater. 339, 354–367.

Zhang, C., Lai, C., Zeng, G., Huang, D., Yang, C., Wang, Y., Zhou, Y., Cheng, M., 2016. Efficacy of carbonaceous nanocomposites for sorbing ionizable antibiotic sulfamethazine from aqueous solution. Water Res. 95, 103–112.

Zhang, C., Shan, B., Tang, W., Zhu, Y., 2017a. Comparison of cadmium and lead sorption by *Phyllostachys Pubescens* biochar produced under a low-oxygen pyrolysis atmosphere. Bioresource Technol. 238, 352–360.

Zhang, F., Wang, X., Yin, D., Peng, B., Tan, C., Liu, Y., Tan, X., Wu, S., 2015. Efficiency and mechanisms of Cd removal from aqueous solution by biochar derived from water hyacinth (Eichornia crassipes). J. Environ. Manag. 153, 68–73.

Zhang, T., Zhu, X., Shi, L., Li, J., Li, S., Lü, J., Li, Y., 2017b. Efficient removal of lead from solution by celery-derived biochars rich in alkaline minerals. Bioresour. Technol. 235, 185–192.

Zhao, N., Yang, X., Zhang, J., Zhu, L., Lv, Y., 2017. Adsorption mechanisms of dodecylbenzene sulfonic acid by corn straw and poplar leaf biochars. Materials 10 (10), 1119.

Zhou, C., Lai, C., Huang, D., Zeng, G., Zhang, C., Cheng, M., Hu, L., Wan, J., Xiong, W., Wen, M., 2017. Highly porous carbon nitride by supramolecular preassembly of monomers for photocatalytic removal of sulfamethazine under visible light driven. Appl. Catal. B Environ. 220, 201–210.

Zhou, L., Liu, Y., Liu, S., Yin, Y., Zeng, G., Tan, X., Hu, X., Hu, X., Jiang, L., Ding, Y., 2016. Investigation of the adsorption-reduction mechanisms of hexavalent chromium by ramie biochars of different pyrolytic temperatures. Bioresour. Technol. 218, 351–359.

Zhou, Q., Liao, B., Lin, L., Qiu, W., Song, Z., 2018. Adsorption of Cu(II) and Cd(II) from aqueous solutions by ferromanganese binary oxide-biochar composites. Sci. Total Environ. 615, 115–122.

Zhuang, Y.T., Gao, W., Yu, Y.L., Wang, J.H., 2016. A three-dimensional magnetic carbon framework derived from Prussian blue and amylopectin impregnated polyurethane sponge for lead removal. Carbon 108, 190–198.